JOURNAL OF PETROLOGY | VOLUME 53 | NUMBER 10 | PAGES 2095–2113 | 2012 | doi:10.1093/petrology/egs045

Picrites from the Emeishan Large Igneous Province, SW China: a Compositional Continuum in Primitive Magmas and their Respective Mantle Sources

VADIM S. KAMENETSKY[1]*, SUN-LIN CHUNG[2], MAYA B. KAMENETSKY[1] AND DMITRI V. KUZMIN[3]

[1]ARC CENTRE OF EXCELLENCE IN ORE DEPOSITS AND SCHOOL OF EARTH SCIENCES, UNIVERSITY OF TASMANIA, HOBART, TASMANIA, AUSTRALIA

[2]DEPARTMENT OF GEOSCIENCES, NATIONAL TAIWAN UNIVERSITY, TAIPEI, TAIWAN

[3]MAX PLANCK INSTITUTE FOR CHEMISTRY, POSTFACH 3060, 55020 MAINZ, GERMANY

RECEIVED JULY 20, 2011; ACCEPTED JUNE 8, 2012
ADVANCE ACCESS PUBLICATION AUGUST 8, 2012

Flood basalts are one of the remaining enigmas in global mantle petrology. They come in enormous quantities of up to 10^6 km^3 of mantle-derived melt, and they erupt in rather short time intervals of only a few million years. Throughout geological history, all continents have been periodically flooded by dominantly basaltic and rare picritic magmas that can differ widely within the same province in terms of their major element (e.g. high- and low-Ti series), trace element, and radiogenic isotope compositions, suggesting significant compositional heterogeneity within the mantle source regions tapped. In this study of the Late Permian Emeishan large igneous province (ELIP) in SW China picrite lavas from thick stratigraphic successions at Binchuan and Yongsheng represent the low-Ti and high-Ti 'classic' end-members of continental flood basalt magmatism, respectively. This study focuses on the petrochemical variability of the Emeishan magmas, and the genetic links between the suites and their respective mantle sources, based upon estimates of the chemical compositions of the primary melts represented by homogenized melt inclusions hosted by exceptionally primitive olivine (up to 92 mol % Fo in both suites) and Cr-spinel (Cr# 64–72 mol % in Binchuan and 65–80 mol % in Yongsheng) phenocrysts. The average compositions of the melt inclusions and their overall chemical variability, together with the presence of picrites in the province (e.g. Lijiang and Dali localities) with compositions intermediate between the low- and high-Ti end-members, suggest that numerous parental magma batches contributed to a diverse spectrum of more differentiated basaltic magmas within the ELIP. The end-member and intermediate magma compositions are confirmed by the compositions of phenocrysts (Ni and Mn abundances in olivine, Ti abundances in Cr-spinel and clinopyroxene, and trace element abundances in clinopyroxene). The end-member melt and phenocryst compositions (e.g. Gd/Yb in bulk-rocks, melt inclusions and clinopyroxene and Ni–Mn systematics in olivine) suggest a peridotite and garnet pyroxenite mantle source for the low- and high-Ti end-members, respectively. The Sr and Nd isotopic compositions of the two end-member magmas are similar [$^{87}Sr/^{86}Sr_i \sim 0{\cdot}7045$; $\varepsilon Nd(t) \sim +1{\cdot}7$] and are considered to reflect a source in the subcontinental lithospheric mantle rather than the convective asthenosphere or a deep mantle 'plume'.

KEY WORDS: *Emeishan; flood basalts; lithosphere; melt inclusions; olivine*

INTRODUCTION

Throughout geological history all of the continents have been periodically flooded within time-scales of only a few million years by enormous amounts (>10^5 km^3) of basaltic

*Corresponding author. Telephone: +61362267649.
E-mail: Dima.Kamenetsky@utas.edu.au

and picritic magmas (Coffin & Eldholm, 1992; http://www.largeigneousprovinces.org/). The large volumes and short durations of the flood magmatism resulting in large igneous provinces (LIPs) have yet to be satisfactorily explained, and the mantle sources of such voluminous magmas are still debated. For mantle-derived magmatism of such magnitude the majority of the basalts forming the LIPs are relatively evolved, as manifested by their low MgO (<8 wt %) contents and absence or rarity of olivine phenocrysts. When the latter are present, highly forsteritic (Fo) compositions, analogous to mantle values, can be lacking in the most typical picrites (e.g. Siberia; Sobolev *et al.*, 2009). This makes the search for primary melts difficult, if not impossible. However, picritic rocks that contain forsteritic olivine are observed occasionally in some LIPs (e.g. Emeishan; see review by Hanski *et al.*, 2010), and are more common in others, such as Karoo (Cox & Jamieson, 1974) and West Greenland (Holm *et al.*, 1993), suggesting the existence of high-Mg, peridotite-equilibrated magmas that were parental to the dominant basaltic magmas.

The Late Permian Emeishan large igneous province (ELIP) in SW China contains a succession of multiple lava units with an overall thickness reaching 5 km (e.g. Chung & Jahn, 1995; Xu *et al.*, 2001). The basaltic rocks belonging to each magmatic pulse are characteristically homogeneous, whereas different units in the same region can differ widely in their major element composition (e.g. high- and low-Ti series), trace element abundances and radiogenic isotope ratios (e.g. Xu *et al.*, 2001; Zhou *et al.*, 2008). The occurrence of geochemically diverse units in different spatial and stratigraphic positions is conventionally interpreted to reflect either melting of a single mantle source at different pressures and temperatures or a contribution from several discrete mantle sources (e.g. Song *et al.*, 2001; Xu *et al.*, 2001, 2007; Xiao *et al.*, 2004; Zhang *et al.*, 2006*b*; Wang *et al.*, 2007; He *et al.*, 2010; Li *et al.*, 2010; Shellnutt & Jahn, 2011). Existing models for the ELIP, however, do not take into account the possibility that basaltic magmas may result from mixing of different melt batches in the magmatic plumbing system, and as such they may have numerous 'parents' (i.e. melts from which the resultant chemical characteristics of rocks are inherited). Such parental magma compositions may have primary melts among their precursors (i.e. melts that equilibrated with their mantle source at the time of melt segregation). Recognition and classification of the mantle sources and their respective melting conditions ultimately rely on the characteristics of these primary melts.

This study aims to identify the range of the ELIP near-primary melts using the compositions of the least evolved, picritic rocks in the province and their phenocryst assemblages, which include primitive olivine, Cr-spinel and clinopyroxene. Studies of melt inclusions are used to test whether the studied rocks are representative of primary melt compositions. The integration of picritic whole-rock, mineralogical and melt inclusion data, together with previously published radiogenic isotope data, suggests a continuous range in melt compositions and the involvement of diverse mantle sources.

EMEISHAN LARGE IGNEOUS PROVINCE

The ELIP is located in the western margin of the Yangtze craton in SW China, comprising a continental flood basalt province covering an area of >250 000 km^2 and having a total volume of $>0{\cdot}3 \times 10^6$ km^3 (Chung & Jahn, 1995; Xu *et al.*, 2001; Hanski *et al.*, 2010). In the past decade, the ELIP has been the focus of numerous investigations and is one of the most comprehensively studied LIPs in the world. The Emeishan volcanism was coincident with the end-Guadalupian (~260 Ma) mass extinction (Zhou *et al.*, 2002; Xu *et al.*, 2008). Mafic–ultramafic intrusions within the ELIP are the host of world class Fe–Ti–V oxide deposits and Ni–Cu–PGE sulfide deposits. The ELIP is also considered to be one of the best examples of a mantle plume generated LIP, although this has been challenged by some workers (e.g. Shellnutt *et al.*, 2010). The ELIP was dissected by Mesozoic and Cenozoic faulting associated with complex tectonic events and block movements in SE Asia, among which the collision of India with Eurasia may have played the most significant role (Chung *et al.*, 1997). Consequently, the ELIP is bordered to the south by the sinistral Ailao Shan–Red River shear zone, which runs in a NW–SE direction from SW China to northern Vietnam (Fig. 1). Late Permian volcanic rocks that can be correlated with those exposed in the ELIP have been reported in regions south of the shear zone; for example, in the Jinping area close to the China–Vietnam border and the Song Da zone of northern Vietnam (Song *et al.*, 2004; Wang *et al.*, 2007; Tran *et al.*, 2011).

Picrite samples

The principal samples in this study are olivine-phyric extrusive rocks (hereafter termed picrites) with >16 wt % MgO, from Yongsheng [EM55, EM57 and EM58 from Chung & Jahn (1995)] and Binchuan [EM43 from Xu *et al.* (2001)], at the western margin of the ELIP (Fig. 1). Additional picrite samples from nearby localities at Lijiang and Dali (Fig. 1; Hanski *et al.*, 2010) are also considered in this study in more detail than other previously reported Emeishan rocks. At Yongsheng the samples were collected from different levels of a 50 m thick lava flow within a 1–2 km thick volcanic sequence (Chung & Jahn, 1995). At Binchuan the studied picritic lavas occur among basalts and andesites in the upper part of an exceptionally thick (>5 km) succession, within a geochemical transition to more enriched basaltic and more evolved rocks

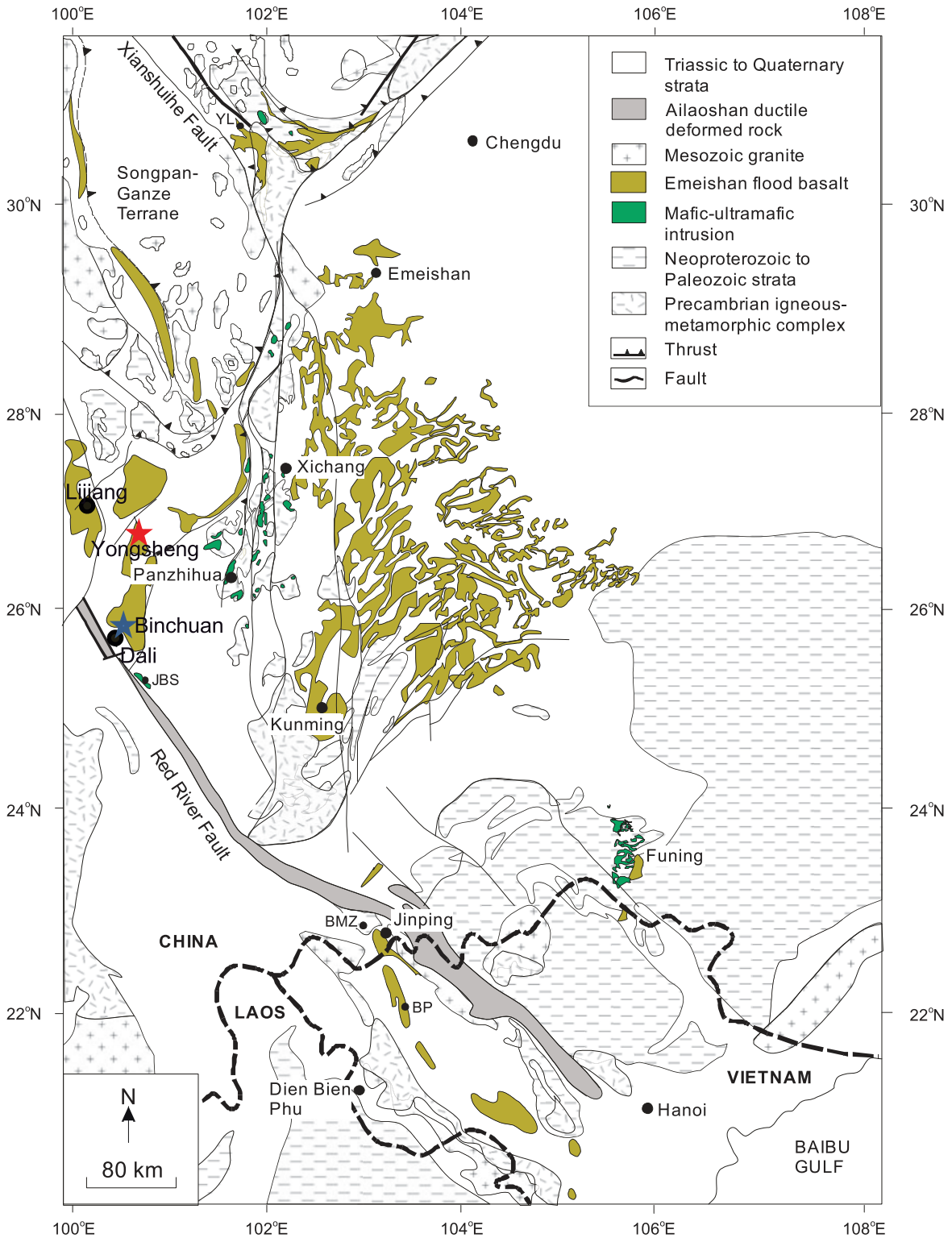

Fig. 1. Distribution of volcanic and intrusive rocks in the Emeishan large igneous province, SW China. Locations of picrites reported in this study [Binchuan and Yongsheng; see also Xu *et al.* (2001) and Chung & Jahn (1995), respectively] and other studies (Lijiang and Dali; Hanski *et al.*, 2010) are indicated.

(Xu *et al.*, 2001). Other picrites have been reported from locations ~1·3 km stratigraphically lower in the Binchuan sequence (Xiao *et al.*, 2004). However, we note that the Asian monsoonal climate conditions in the region, which have led to intense weathering of rock exposures, combined with the tectonic disruption make correlations between the different localities and duplicate sampling very difficult.

All the studied samples are massive, moderately fresh rocks with euhedral olivine phenocrysts containing abundant Cr-spinel and melt inclusions (Fig. 2). The Binchuan picrite has a vesicular microcrystalline to glassy groundmass in which large olivine (up to 3 mm) and Cr-spinel (up to 0·4 mm) phenocrysts are present. The olivine is strongly fractured and serpentinized along fractures. Clinopyroxene and plagioclase phenocrysts are rare. In contrast, the Yongsheng picrites contain less altered olivine and ~15–20% zoned clinopyroxene phenocrysts (up to 5 mm), often containing round inclusions of olivine. The fine-grained groundmass is composed of plagioclase, clinopyroxene, phlogopite, apatite and Fe–Ti oxide minerals.

ANALYTICAL METHODS

Several thousand olivine grain fragments (0·2–0·5 mm) were separated from crushed chips of the four picrite samples studied and examined individually under a binocular microscope for the presence of unaltered and large (>30 μm) melt inclusions. Such inclusions were found in sufficient quantities in the Yongsheng olivines (Fig. 2e and f), whereas rare preserved melt inclusions in the Binchuan olivine appeared unsuitable for study. Instead, the focus was redirected to the abundant Cr-spinel crystals in the Binchuan picrite following the approach of Kamenetsky (1996). Although melt inclusions in Cr-spinel cannot be observed in transmitted light owing to the opacity of the host, reflected light microscopy on polished surfaces revealed numerous melt inclusions (Fig. 2b and c). The melt inclusions in both olivine and Cr-spinel have a negative crystal shape and consist of glass, pyroxene microlites, vapour bubble(s) and occasionally sulphide globules. Heating and quenching was employed to convert the melt inclusions into glass. The temperature of complete melting in the olivine-hosted inclusions was determined from several heating experiments with visual control. The olivine and chromite grains and a piece of graphite were wrapped in Pt foil, heated in a vertical furnace with a flow of pure Ar gas at 1320°C for 6 min, and then quenched in water. The epoxy-mounted grains were polished to expose homogenized melt inclusions for *in situ* analysis by microbeam techniques.

Major elements in minerals and glasses were analysed using a JEOL Superprobe JXA-8200 electron microprobe (Max Planck Institute for Chemistry, Mainz, Germany). We applied a 15 kV accelerating voltage, 12 nA electron beam current and a defocused 5 μm beam for analyses of olivine-hosted glass inclusions. Conditions of 20 kV and a 20 nA primary beam current were used for analyses of spinel inclusions in olivine and clinopyroxene. Olivine was analysed at an accelerating voltage of 20 kV and a beam current of 300 nA, following a special procedure that allows 20–30 ppm (2σ error) precision and accuracy for Ni, Ca, Mn, Al, Ti, Cr and Co, and 0·02 mol % for the forsterite component in olivine (Sobolev *et al.*, 2007). Peak counting times on major elements were 60 s and 30 s for the background. The standard built-in ZAF correction routine was used. Trace element concentrations in melt inclusions were analysed by laser ablation inductively coupled plasma mass spectrometry at the University of Tasmania. This instrumentation comprises a New Wave Research UP213 Nd–YAG (213 nm) laser coupled to an Agilent 4500 quadrupole mass spectrometer. For this study, analyses were performed in a He atmosphere by ablating 20–70 μm diameter spots at a rate of five shots per second using a laser power of ~12 J cm^{-2}.

WHOLE-ROCK COMPOSITIONS

Chemical classification of continental flood basalts worldwide and the ELIP rocks in particular (Xu *et al.*, 2001; Xiao *et al.*, 2004) is traditionally based on the TiO_2 content or the Ti/Y ratio. The latter reduces the effects of crystal fractionation, especially in the more primitive compositions, before fractionation of Ti-bearing oxides, such as magnetite and ilmenite, becomes significant. The boundary between so-called low-Ti and high-Ti rocks in the ELIP has been drawn at Ti/Y = 500 (Xu *et al.*, 2001). The studied picrites have significantly different Ti/Y ratios that represent the lowest (~300, Binchuan) and highest (~800, Yongsheng) values for the whole province (Fig. 3; Supplementary Data, Electronic Appendix 1, available for downloading at http://www.petrology.oxfordjournals.org). Picrites from other ELIP localities have intermediate and distinct Ti/Y ratios that place them on both sides of the Ti/Y boundary, with rocks from Dali (360–395) having more affinity with the Binchuan low-Ti end-member, whereas the Lijiang picrites (630–700) are closer to the Yongsheng high-Ti end-member (Fig. 3). The Ti/Y values are positively correlated with Gd/Yb, a ratio that is commonly used to constrain the presence of residual garnet in the mantle source.

Olivine accumulation (see below) in the studied picrites strongly controls the whole-rock MgO contents, whereas the abundances of elements incompatible in olivine (e.g. TiO_2) can be compared at a given MgO content (Fig. 4; Electronic Appendix 1). Olivine accumulation or fractionation trends on the MgO vs TiO_2 diagram (Fig. 4), drawn through the Binchuan and Yongsheng picrite compositions, encompass all the basalt and picrite compositions in the province. Notably, the overall range

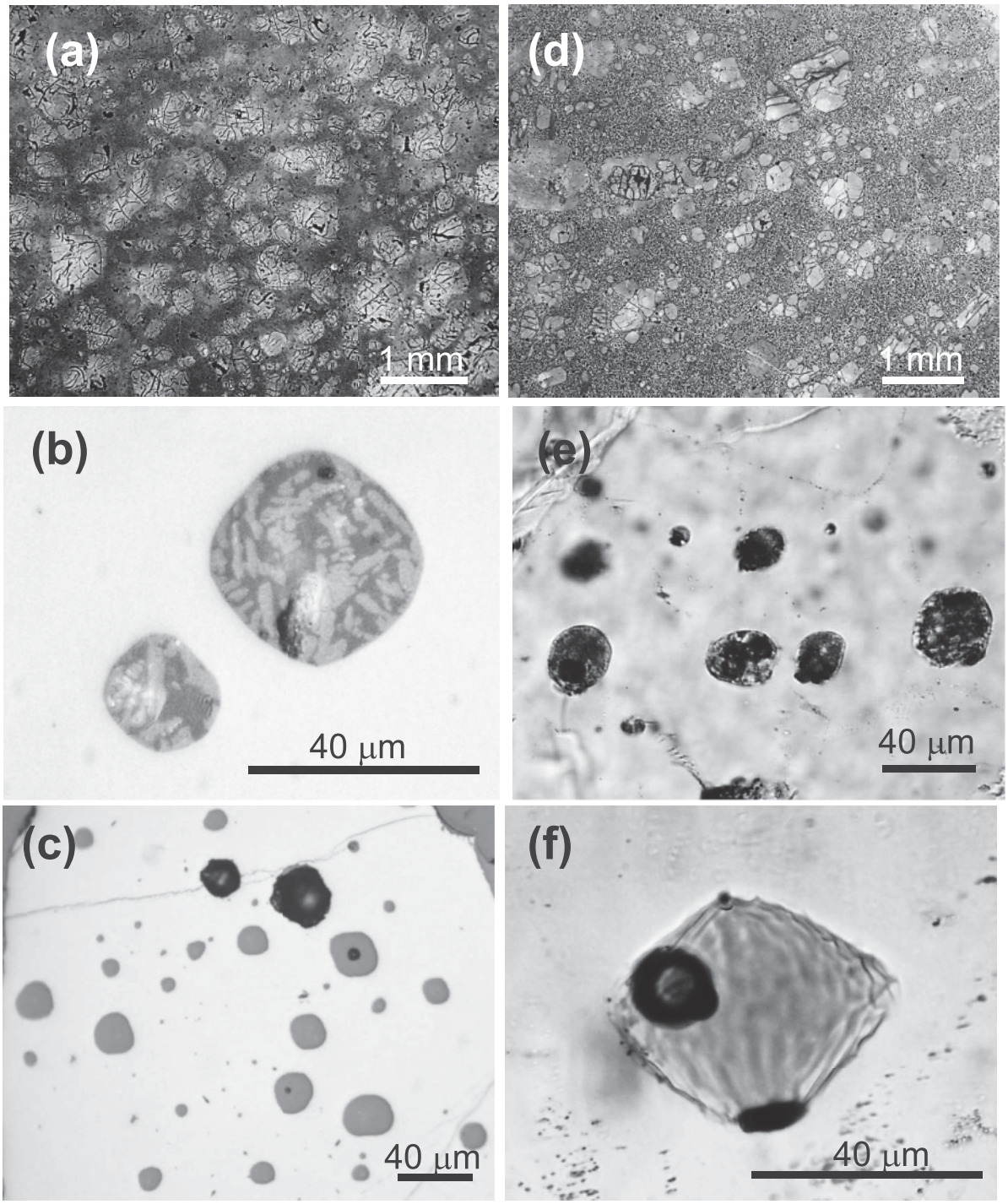

Fig. 2. Photomicrographs showing textural characteristics (a, d), unhomogenized melt inclusions (b, e), and homogenized melt inclusions (c, f) in the Emeishan low-Ti (Binchuan area) and high-Ti (Yongsheng area) picrites, respectively. The host minerals of the melt inclusions are Cr-spinel (b, c; reflected light) and olivine (e, f; transmitted light).

in TiO_2 does not change over the range of MgO abundances, at least to the start of the olivine–clinopyroxene cotectic estimated to occur at ~10–11 wt % MgO from CaO variations. The low-Ti and high-Ti end-member compositions (hereafter LTi and HTi, respectively), defined by the studied picrites and their hypothetical derivative magmas, have different abundances of other olivine-incompatible major elements. In particular, CaO

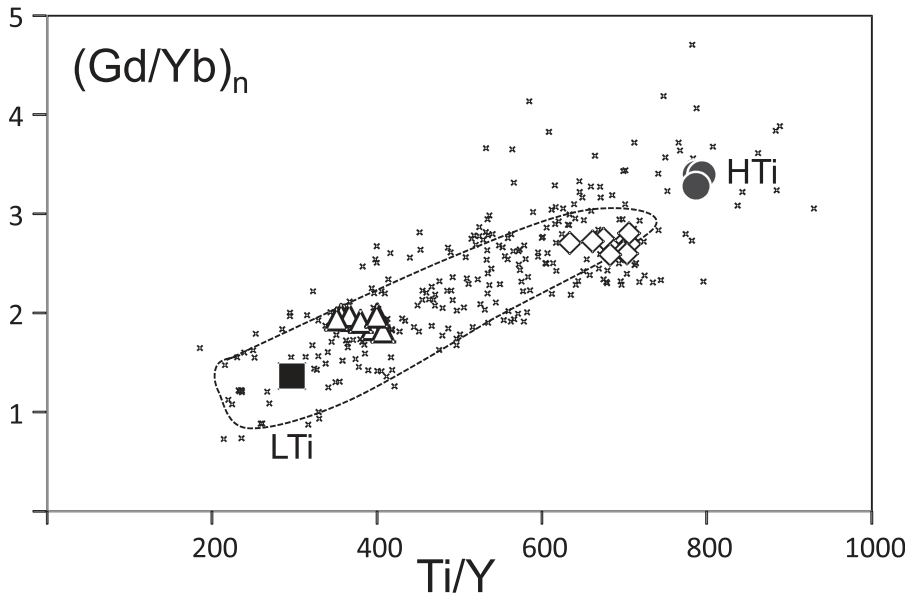

Fig. 3. Relationships between the 'classification' parameters Ti/Y and $(Gd/Yb)_n$ [normalization to the primitive mantle composition of Sun & McDonough (1989)] for the low-Ti (squares, Binchuan area; this study), high-Ti (circles, Yongsheng area; this study), intermediate-Ti (triangles, Dali area; diamonds, Lijiang area; Hanski *et al.*, 2010) picrites and other picritic and basaltic rocks (small crosses; Chung & Jahn, 1995; Song *et al.*, 2001, 2003, 2004, 2006, 2008; Xu *et al.*, 2001, 2007; Xiao *et al.*, 2003, 2004; Zhang *et al.*, 2006*a*; Wang *et al.*, 2007; Qi *et al.*, 2008; He *et al.*, 2010; Li *et al.*, 2010) from the Emeishan large igneous province. Dashed field shows the range of basaltic glasses from mid-ocean ridges (after Kamenetsky *et al.*, 2000; le Roux *et al.*, 2002; Sun *et al.*, 2008).

and Al_2O_3 contents are higher in the LTi, whereas olivine-compatible Ni is lower (Fig. 4). The lithophile trace elements plotted on a 'primitive mantle'-normalized diagram (Fig. 5) also show principal differences between the two end-members: the heavier rare earth elements (HREE) from Eu to Lu are strongly fractionated (by a factor of 4·4) in the HTi suite, whereas normalized abundances of these elements remain almost constant in the LTi suite. The LTi samples, however, demonstrate an increase in fractionation among the light REE [LREE; $(La/Sm)_n = 3$], similar to the extent of LREE fractionation in the HTi picrites (Fig. 5). The picrites from the Dali area with intermediate Ti/Y and Gd/Yb (hereafter ITi, Fig. 3) have less fractionated LREE than both the LTi and HTi end-members [$(La/Sm)_n = 2·2$; Fig. 5].

PRIMITIVE LIQUIDUS ASSEMBLAGE

Olivine

Olivine phenocryst compositions in the studied picrites are highly variable in terms of their forsterite content (Fo). Significant ranges in Fo in a single rock (83–91 mol % in LTi and 79–91·6 mol % in HTi, Fig. 6, Electronic Appendix 2) are accompanied by systematic changes in the first row transition elements in the bulk-rocks (e.g. Ni, Co, and Cr; Fig. 4), consistent with olivine (plus Cr-spinel) fractional crystallization of the melt from which the olivine crystallized. These processes are reflected in a NiO and Cr_2O_3 decrease and MnO increase in both the LTi and HTi suites as Fo decreases (Fig. 7, Electronic Appendix 2). Such variations in Fo content, coupled with systematic behaviour of the trace elements, indicate that the olivine phenocrysts in this study formed during prolonged crystallization of primitive melts, accumulated in the plumbing system, and were delivered to the surface without re-equilibration with the transporting melt, which was more evolved than the melts from which the olivine crystallized.

The observed mixed populations of olivine phenocrysts are represented by the majority of the Fo-rich compositions in the LTi picrites (>88 mol % Fo) compared with the HTi picrites where less forsteritic olivine is dominant (82–86 mol %, Fig. 6). The distinctions in average olivine compositions (Fig. 6) and the amount of accumulated olivine influence the MgO content of the whole-rocks (Fig. 4). Statistically, however, the more magnesian olivine in the LTi picrites does not imply that their primary melts had higher Mg/Fe. The abundances of the trace elements in olivine from the LTi and HTi picrites, although varying systematically with Fo, are distinct: the HTi olivines have the highest Ni and lowest Mn contents, whereas the LTi olivines have markedly lower Ni and higher Mn contents at any given value of Fo (Fig. 7). The LTi olivines are also systematically higher in Ca, Co and Al, but lower in Cr at a given Fo content (Electronic Appendix 2).

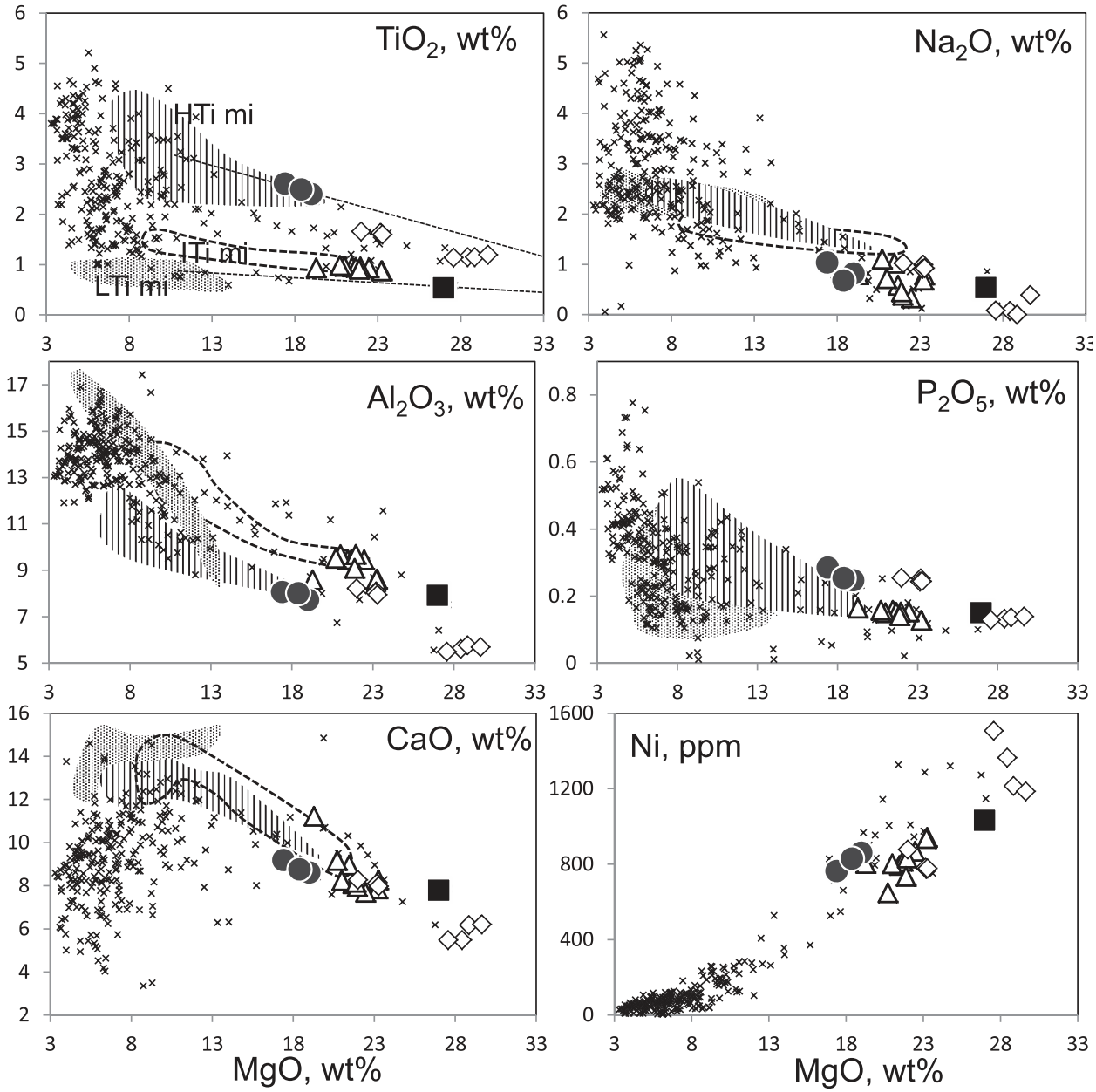

Fig. 4. Major (TiO_2, Al_2O_3, CaO, Na_2O, P_2O_5) and trace (Ni) element variations vs MgO in the Emeishan rocks and homogenized melt inclusions [shown by fields; LTi mi and HTI mi (this study); ITi mi from sample 1A-EJH-06, Dali (Hanski *et al.*, 2010)]. Trend lines correspond to subtraction or accumulation of the average olivine from whole-rock LTi and HTi picrite compositions. The trends are projected to points where clinopyroxene joins olivine on the liquidus (~10 wt % MgO, estimated from inflection of Sc trends). Melt inclusions in olivine are recalculated to be in equilibrium with the host olivine using the petrogenetic models of Ford *et al.* (1983) and Danyushevsky *et al.* (2000) and the Petrolog software (Danyushevsky, 2001) All compositions are normalized to 100 wt %. Symbols and data sources as in Fig. 3. The compositional data for the picrites and melt inclusions are given in Electronic Appendices 1 and 5.

The olivine population in the picrites with intermediate Ti/Y values (hereafter ITi, samples 1a-EJH-06, 7-EJH-08, 13-EJH-08; Hanski *et al.*, 2010) contains even more primitive compositions than the end-member picrites, with Fo contents varying between 82 and 93·5 mol % (Electronic Appendix 2). The 'intermediate' character of these rocks is confirmed by the olivine NiO and MnO abundances, which are clearly transitional between those in the LTi and HTi olivines (Fig. 7).

Chromian spinel

Cr-spinel is present as olivine-hosted inclusions (in both LTi and HTi picrites) and microphenocrysts in the groundmass of the LTi picrite. The Cr-spinel inclusions

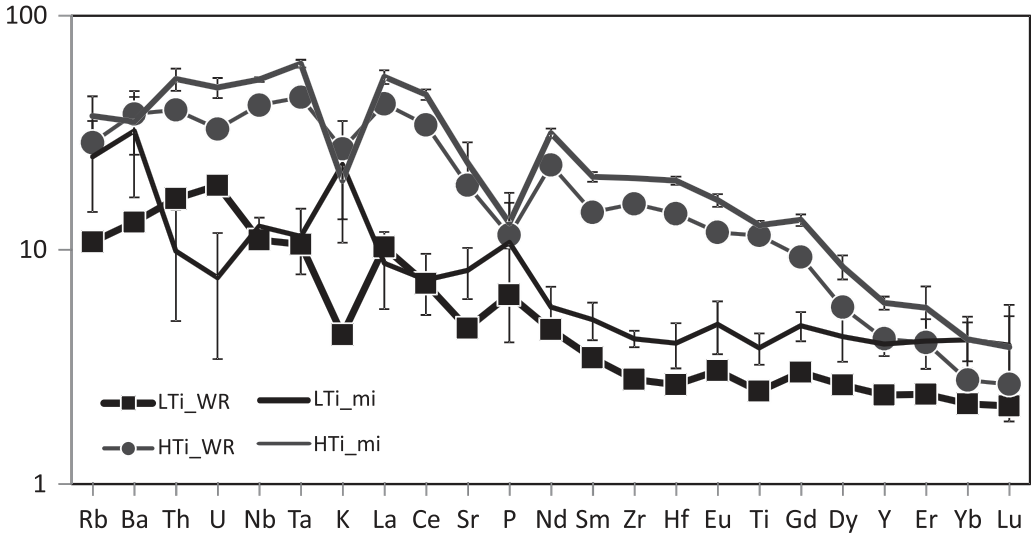

Fig. 5. Primitive mantle-normalized (after Sun & McDonough, 1989) average trace element compositions of the average low-Ti and high-Ti picrites and homogenized melt inclusions (bars show one standard deviation) in the same samples. The trace element data are given in Electronic Appendices 1 and 5.

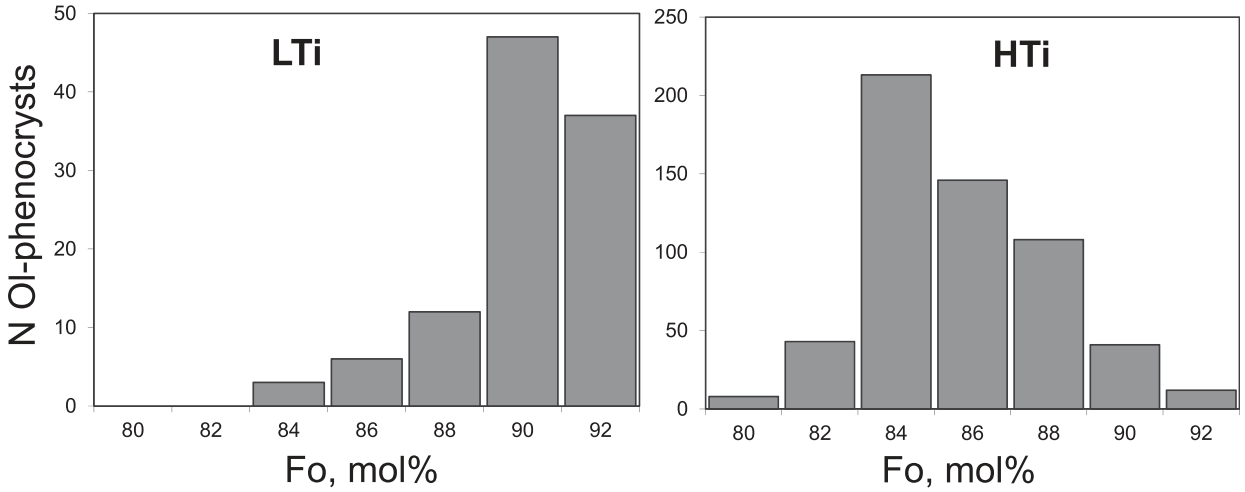

Fig. 6. Histograms showing the distribution of forsterite (Fo) contents in olivine phenocryst populations. The full dataset is given in Electronic Appendix 2.

are in equilibrium with the host olivine as manifested by the positive correlation between the Mg# [Mg/(Mg + Fe^{2+})] of the inclusions and the host olivine (Fig. 8a). The Cr-spinel compositions in the LTi picrite are characterized by significantly lower TiO_2 contents (0·5–0·7 wt %) compared with those in the HTi picrites (2–6 wt % TiO_2; Fig. 8b; Electronic Appendix 3). The Al_2O_3 contents are also principally different—the spinels in the LTi picrite having a range from 12 to 18 wt %, whereas the HTi chromites have less variable and lower Al_2O_3 (8–10 wt %; Fig. 8b; Electronic Appendix 3). The clear compositional differences between the Cr-spinels in the two end-member picrite suites indicate contrasting parental melt compositions, at least in terms of their TiO_2 and Al_2O_3 contents (Kamenetsky *et al.*, 2001*a*). Based on the spinel compositions the parental melts of the LTi suite were inferred by Kamenetsky *et al.* (2001*a*) to contain ~1 wt % TiO_2 and ~13 wt % Al_2O_3 and those of the HTi suite ~2·5–4 wt % TiO_2 and ~10 wt % Al_2O_3. These estimates are consistent with the compositions of the melt inclusions in the same samples (see below; Fig. 4).

Clinopyroxene

Clinopyroxene phenocrysts in both suites are primitive in composition, and their Mg#s correlate with the Fo contents of olivine in the same samples. Clinopyroxenes from

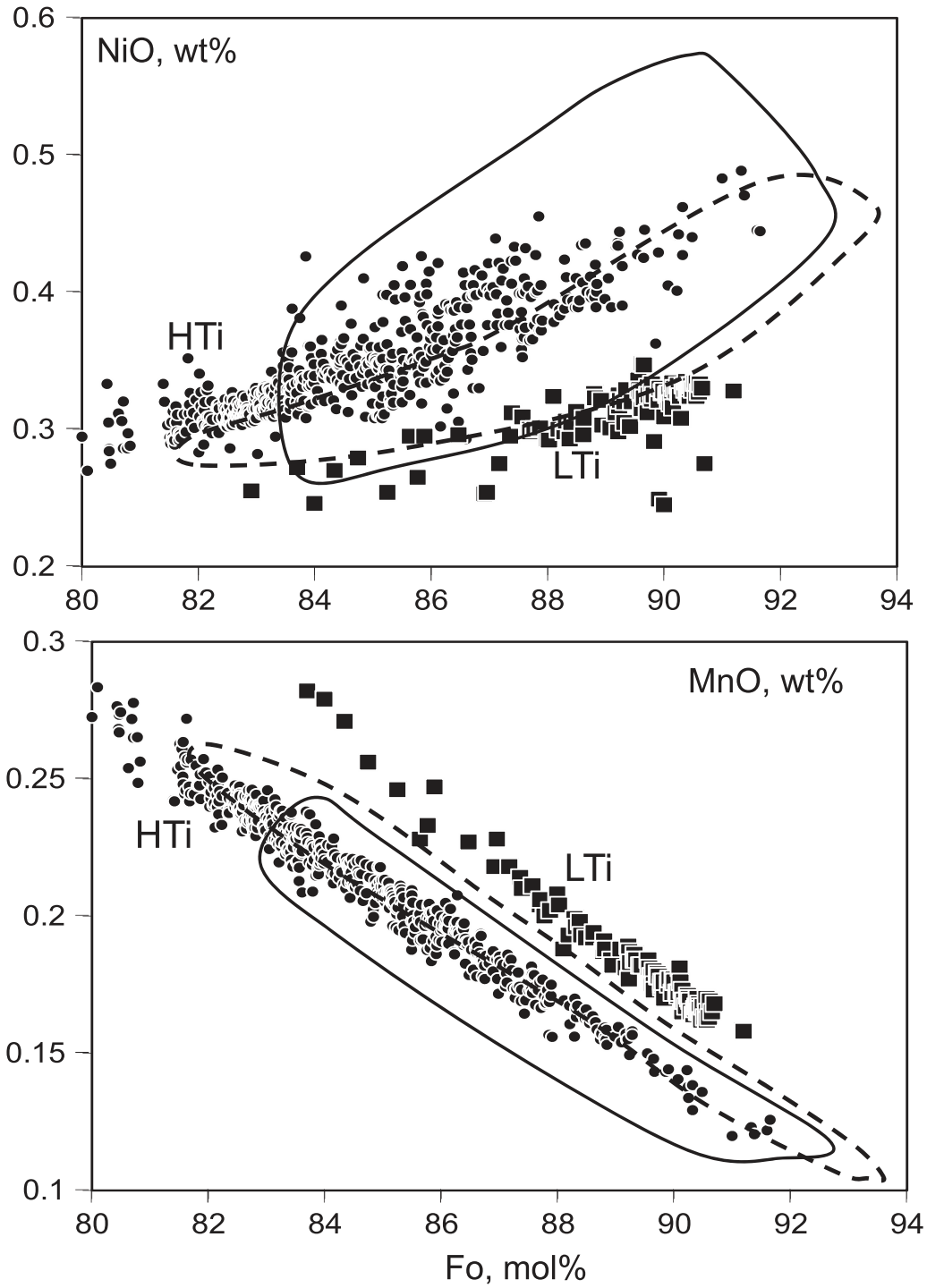

Fig. 7. Relationships between the forsterite (Fo) content and trace element (NiO, MnO) contents of olivine phenocrysts. Fields depicting the compositions of ITi olivines (dashed line; Hanski *et al.*, 2010) and primitive olivines (>84 mol % Fo) from other flood basalt provinces (continuous line; Sobolev *et al.*, 2007) are shown for comparison. Olivine compositions are given in Electronic Appendix 2.

the LTi picrite are more magnesian than those from the HTi rocks (Mg# 88·5–90 mol % vs 84–86 mol %, respectively), and thus element concentrations at the same Mg# cannot be confidently compared. Similar to the observed differences in the whole-rocks and Cr-spinel, the TiO_2 content in clinopyroxene from the HTi picrites is higher by a factor of four than in the LTi suite (Fig. 9a; Electronic Appendix 4). The less magnesian HTi

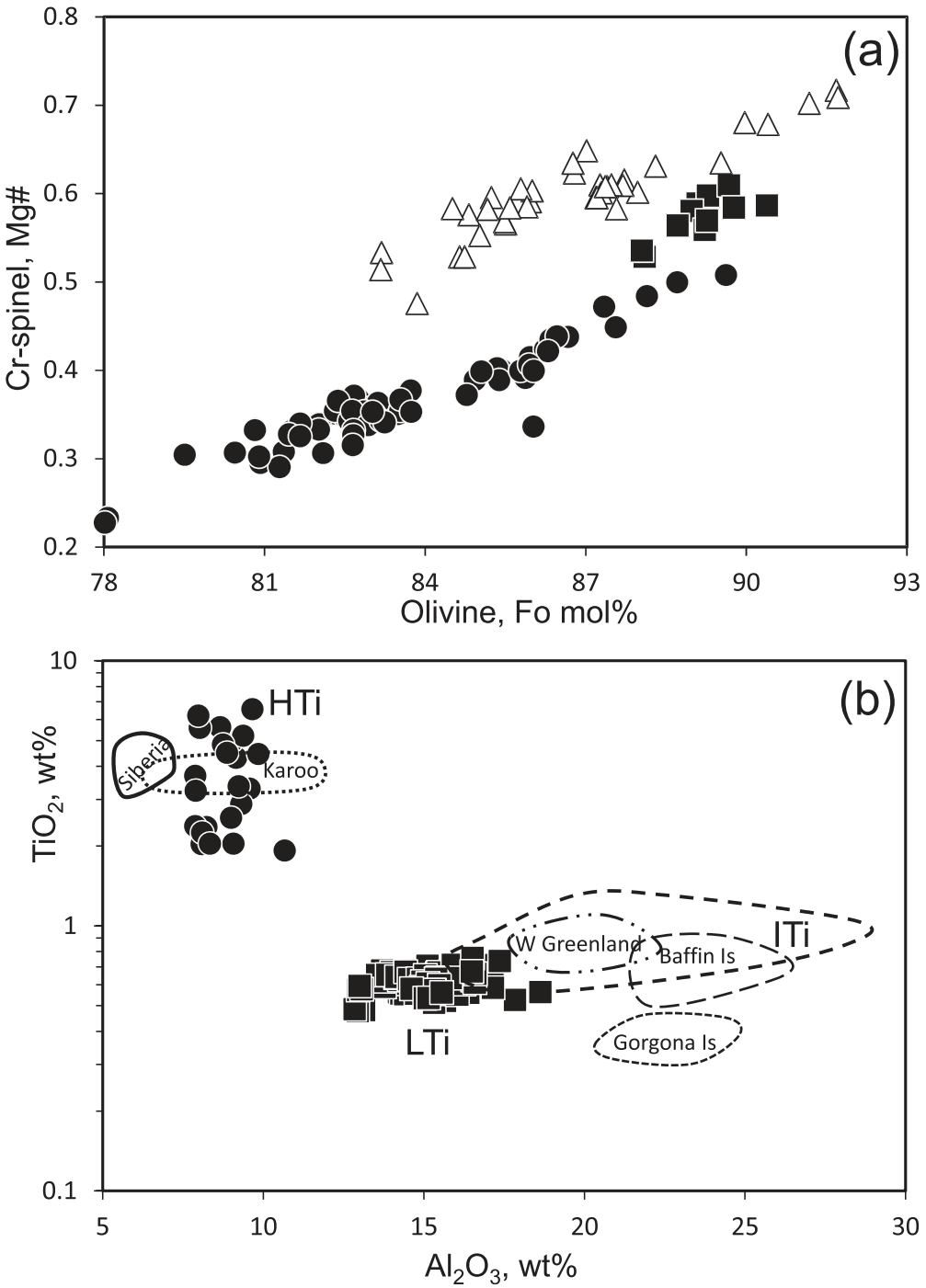

Fig. 8. Relationships between the compositions of Cr-spinel inclusions (Mg#) and host olivine (Fo mol %) phenocrysts (a) Al_2O_3 vs TiO_2 for Cr-spinel associated with the most primitive olivine (>84 mol % Fo) (b) in the Emeishan picrites. Symbols as in Fig. 3. The fields of Cr-spinel in ITi picrites (Hanski *et al.*, 2010) and picrites from other LIPs (Kamenetsky *et al.*, 2001*a*, 2010; Yaxley *et al.*, 2004) are shown for comparison. Cr-spinel compositions are given in Electronic Appendix 3.

clinopyroxene is more Ni-rich (400–450 ppm) than the LTi clinopyroxene with higher Mg# (375–400 ppm Ni, Fig. 9b). All incompatible elements are systematically higher in the HTi clinopyroxene, although there is some convergence of abundances of elements more compatible than Ti (Fig. 10; Electronic Appendix 4). In general, the trace element patterns of the clinopyroxenes resemble those of the corresponding host-rocks (compare Fig. 10

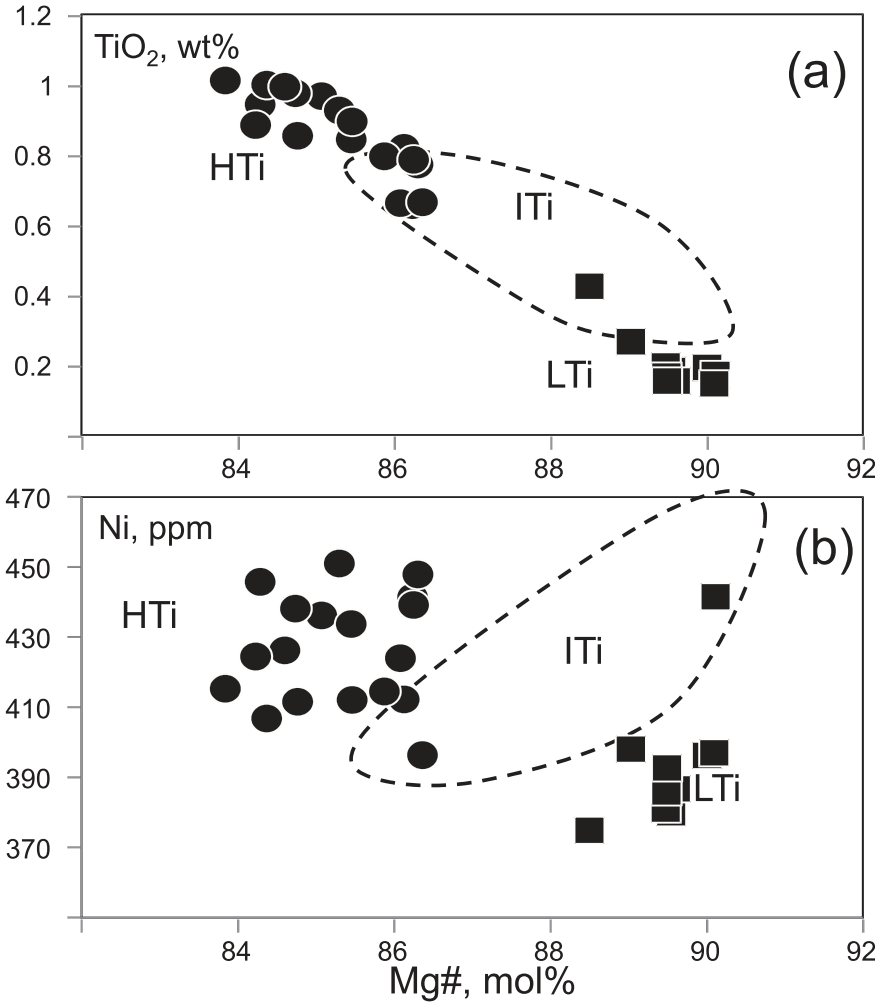

Fig. 9. Representative compositions of clinopyroxene phenocrysts in the Emeishan picrites. Symbols as in Fig. 3. The dashed field shows ITi clinopyroxenes (Hanski *et al.*, 2010). Clinopyroxene compositions are given in Electronic Appendix 4.

and Fig. 5), and can be used to calculate parental melt compositions, provided an appropriate set of partition coefficients is available. The major and trace element compositions of clinopyroxene from the ITi picrite are transitional between those from the LTi and HTi suites (Figs 9 and 10; Electronic Appendix 4).

Melt inclusions

The rehomogenized melt inclusions in olivine are represented by a brownish glass, often with a vapour bubble (<2 vol. %), a sulphide globule, and sometimes an accidently trapped Cr-spinel crystal of variable size (Fig. 2f). The exposed spinel-hosted inclusions appear as homogeneous glass (Fig. 2c). These inclusions with unmelted crystals, large bubbles and intersected by cracks were considered to be compromised, and thus excluded from further analysis.

Sulphide globules in the olivine-hosted melt inclusions from the HTi picrites are volumetrically proportional to the size of the host glass, and thus represent a daughter phase that formed during cooling as a result of the so-called 'Fe loss' process, caused by post-entrapment crystallization and re-equilibration with the host olivine (Danyushevsky *et al.*, 2000, 2002). The 'Fe loss', observed in all olivine-hosted melt inclusions, is greater in more magnesian olivine hosts. Consequently, the measured melt compositions were corrected to account for Fe loss using the method of Danyushevsky *et al.* (2000) and recalculated to be in equilibrium with the host olivine applying the model of Ford *et al.* (1983) using Petrolog software (Danyushevsky, 2001). Any Fe loss that may have also occurred in the spinel-hosted melt inclusions is considered insignificant (Kamenetsky *et al.*, 2002).

The corrected compositions of the melt inclusions and their host minerals are reported in Electronic Appendix 5 and in Figs 3–5. The melt inclusions exhibit specific geochemical characteristics also present in the whole-rock

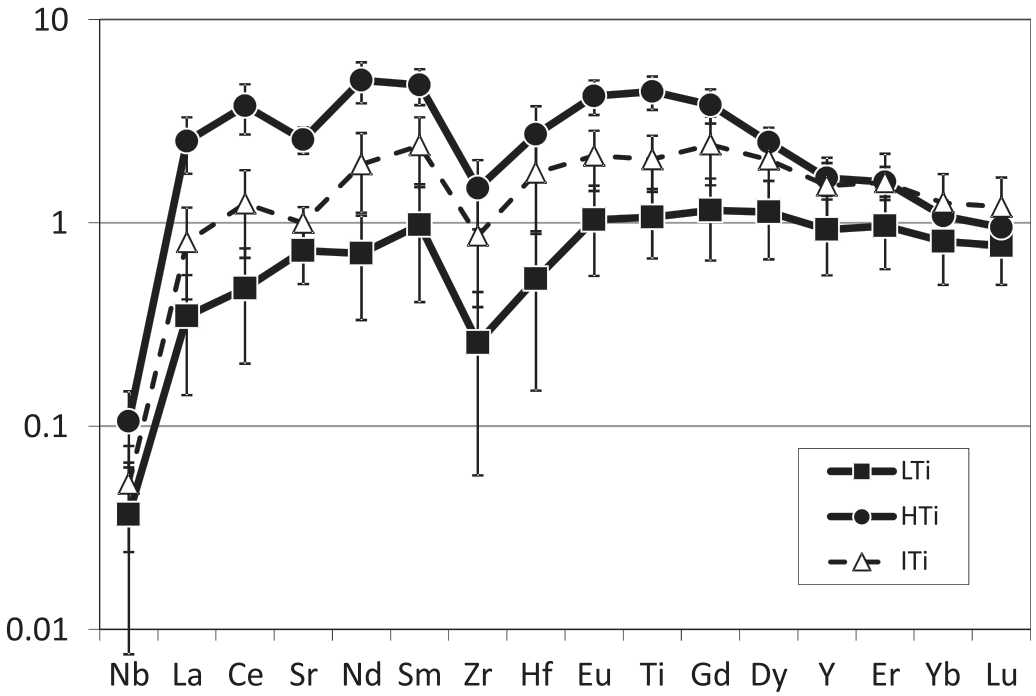

Fig. 10. Average primitive mantle normalized trace-element compositions of clinopyroxene phenocrysts in the Emeishan picrites. Symbols as in Fig. 3. Clinopyroxene compositions are given in Electronic Appendix 4.

compositions; in particular, the distinctive TiO_2 contents and Ti/Y ratios used in the classification of the whole-rock analyses. The hypothetical olivine fractionation or accumulation trends, drawn through the whole-rock and average olivine phenocryst compositions, intersect the fields of melt inclusions in an MgO vs TiO_2 diagram (Fig. 4). If fractionation of a primary melt is considered, the composition of the LTi picrite is significantly over-enriched in the olivine component compared with the melt inclusions (compare 27 and 14 wt % MgO), whereas the HTi picrite compositions match the most primitive melt inclusions (Fig. 4). Trace element concentrations in the melt inclusions broadly mirror their respective whole-rock compositions. For example, HTi melt inclusions show greater enrichment in incompatible trace elements than those from the LTi (Fig. 5), and the HREE systematics suggest a principal control from residual garnet in the source of the HTi melts (Gd/Yb ~4·0 in HTi compared with ~1·4 in LTi).

The melt inclusions from the ITi picrites (Hanski *et al.*, 2010) correspond well to their host-rock compositions; the latter show no excessive olivine component and thus can be considered similar to primary melts (Fig. 4), except for elements affected by alteration. The most affected elements are alkaline and alkali-earth elements, which can be much lower in the picrites than in the melt inclusions (e.g. Na_2O in all suites and K_2O in LTi) or higher (e.g. K_2O in HTi).

In general, the melt inclusions from each suite show compositional variability at a given MgO content, even above the olivine–clinopyroxene cotectic (>10–11 wt % MgO), where simple olivine control is expected. The concentration ranges are most significant for incompatible lithophile elements such as TiO_2, K_2O, P_2O_5, Cl and REE (2–5 times variation; Electronic Appendix 5). This suggests that the melt inclusions do not belong to the same magmatic differentiation series, implying that they and thus the whole-rock compositions reflect contributions from multiple primitive magma batches mixing with more evolved magmas.

DISCUSSION

Parental melts: compositional end-members

The primary magmas supplying single LIPs are likely to be compositionally variable, reflecting different mantle sources, mantle heterogeneity, variations in melting degree and depth of melt segregation. Additional changes to the primary melt compositions, superimposed on the original variability, may be caused by reaction with both lithospheric mantle and crustal rocks during magma ascent and residence in crustal reservoirs. The original and induced variability of the erupted LIP magmas thus significantly hinders the recognition of the primary melts and their respective mantle sources. The rarity and sometimes absence of primitive magmatic rocks in many provinces further complicates this research.

Our search for the Emeishan primary melts focused on picritic rocks with early crystallizing, high-Fo olivine and Cr-spinel. This helped to overcome compositional effects caused by post-melting processes (e.g. contamination and crystal fractionation). Moreover, the use of homogenized melt inclusions provides the most direct approach to estimating the compositions of the melts that crystallized the most primitive phenocrysts. The rocks selected for this study are not only the most magnesian in the province, but also the most contrasting in terms of their mineral and melt inclusion compositions.

The applied classification scheme based on Ti/Y reveals that the studied magmatic rocks reflect the compositional end-members that are parental to the HTi and LTi series (see also Xu *et al.*, 2001). These series cannot be related to each other by crystal fractionation (Figs 3–5). The compositions of the phenocrysts (Figs 7–9) are characteristic of their distinct parental melts. Despite moderate post-magmatic alteration that has affected some fluid-mobile elements (e.g. Na_2O and large-ion lithophile elements) the whole-rock compositions correspond well to their constituent components, represented by the phenocryst assemblage and the melt inclusions (Figs 3–9). It should be noted that the identification of the exact composition and temperature of the primary magmas is hampered by our inability to recognize the composition of the liquidus olivine at the start of crystallization (for example, the most primitive olivine crystals found in the LTi and HTi picrites are 2·5 and 1·9 mol % Fo less magnesian, respectively, than those in the ITi picrites; Fig. 7), constrain the oxygen fugacity (Fe^{2+}/Fe^{3+} ratio in the melt), choose an appropriate coefficient for the Fe^{2+}–Mg partitioning between olivine and liquid, and quantify the amount of volatiles, especially water, in the melt prior to decompression-induced degassing. Moreover, the chemical variability in the melt inclusions from a single sample (Figs 4 and 5) suggests that multiple batches of primary or parental melt were involved. Nevertheless, the overall spectrum of magmas forming the Emeishan igneous province can be evaluated using available bulk-rock and melt inclusion analyses, and constraints on whether the series are discrete or continuous in composition can be made.

Discrete magma series or a compositional continuum?

The geochemical classification introduced previously for the Emeishan magmas (Xu *et al.*, 2001) allows identification of two discrete magma series (low-Ti and high-Ti) with a few subtypes, based on TiO_2 abundance (2·5 wt %) and Ti/Y = 500 (e.g. Xu *et al.*, 2001; Xiao *et al.*, 2004; Ali *et al.*, 2005; He *et al.*, 2010). This scheme was adopted based on extensive studies of flood basalts in other continental large igneous provinces, where the bimodality of the lavas was established from the systematics of the major elements and immobile high field strength elements, such as Ti, Y, Zr, and Nb [see reviews by Turner & Hawkesworth (1995), Ernst *et al.* (2005) and Bryan *et al.* (2010)]. Discrete low-Ti and high-Ti picritic and basaltic series at different stratigraphic positions have been described in most of the major LIPs; for example, Parana (Peate & Hawkesworth, 1996; Peate *et al.*, 1992, 1999), Karoo (Duncan *et al.*, 1984; Sweeney *et al.*, 1991, 1994; Jourdan *et al.*, 2007), Etendeka (Ewart *et al.*, 2004), Deccan (Melluso *et al.*, 1995, 2006), Siberia (Lightfoot *et al.*, 1993; Sobolev *et al.*, 2009), Ferrar (Molzahn *et al.*, 1996), Columbia River (Chesley & Ruiz, 1998) and West Greenland (Holm *et al.*, 1993; Larsen & Pedersen, 2009). The proportion of the two magma types varies significantly; some provinces are dominated by high-Ti lavas [e.g. Siberia (Sobolev *et al.*, 2009) and Karoo (Sweeney *et al.*, 1991)], whereas the low-Ti type is more abundant in others [e.g. West Greenland (Holm *et al.*, 1993; Larsen & Pedersen, 2009)]. The Emeishan province is characterized by thick low-Ti units at the base of the succession in the west, and a dominance of high-Ti series in the east and in the upper parts of the succession throughout the entire region (Xiao *et al.*, 2003, 2004; Xu *et al.*, 2001).

The subdivision of continental flood basalts into low- and high-Ti suites is critical in assigning specific mantle sources and a specific melting process to their origin. So far, the geochemically distinct magma types have been linked to specific petrogenetic processes; for example, melt supply from the subcontinental lithosphere mantle or deep mantle 'plumes' (Ernst *et al.*, 2005). On the other hand, the possibility of significant mixing of distinct mantle sources and/or interaction between asthenospheric melts and the lithosphere is universally admitted. Thus, any genetic model dealing with the identification of mantle sources and the conditions of melting would necessarily depend on whether the magmatic series are discrete or continuous.

In our study the two contrasting series are identified as end-member compositions (LTi and HTi) among the Emeishan picrites, and given the statistical approach applied (large number of mineral and melt inclusion analyses) and consideration of the published ELIP picrite compositions, 'transitional' between the LTi and HTi end-members, it seems unlikely that there were any parental melts in the province beyond the compositional spectrum reported here (Figs 3 and 4). The compositional range expressed in terms of Ti/Y (Fig. 3) and TiO_2 at a given MgO (Fig. 4) and the absence of 'grouping' at either the low-Ti or high-Ti end argue against bimodality and the compositional 'gaps' inferred in previous studies of Emeishan rocks (e.g. Xiao *et al.*, 2004). Instead, the presence of rocks, both picrites and basalts, with chemical characteristics intermediate between those of the inferred end-members strongly suggests a compositional continuum (in TiO_2 or Ti/Y and other element abundances and

element ratios) over significant ranges of MgO. The intermediate picrites, identified in our study (ITi, Figs 3, 4 and 7–10; see also Hanski *et al.*, 2010), and the other picrites shown in Fig. 4, demonstrate that the Emeishan magmatic event included primitive melts with compositions intermediate between the HTi and LTi end-members. Similar to the picrites, the population of basalt compositions as a whole reflects multiple parents among the primitive (picrite) melt compositions that crystallized olivine + Cr-spinel ± clinopyroxene (Fig. 4). In fact, as the melt inclusion data (Figs 4 and 5; Electronic Appendix 5) suggest, the parental melts are even more diverse than those identified among the whole-rock compositions, as the latter have undergone post-magmatic alteration and the disturbance of fluid-mobile element abundances.

The significant geochemical diversity of magmas erupted in different geotectonic settings on a very small scale (a few km^2 or even a single dredge haul) has been recognized for oceanic pillow-rim glasses (e.g. Sigurdsson *et al.*, 1993; Kamenetsky *et al.*, 2000), and is not unique to the ELIP magmas. We are concerned that the spatial and stratigraphic distributions of the geochemically distinct magma types in the Emeishan province (e.g. Xu *et al.*, 2001; Xiao *et al.*, 2003, 2004; He *et al.*, 2010) are not fully documented and not well understood. For example, sample WL38 (Ti/Y = 338, Electronic Appendix 1) reported by Xiao *et al.* (2004) as a picrite from the Binchuan sequence was expected to correspond to the LTi sample EM43 (Ti/Y = 297; Xu *et al.*, 2001) of this study, but instead it matches better the ITi samples from the Dali area (Ti/Y = 351–408; Hanski *et al.*, 2010). According to the stratigraphic reconstructions, sample WL38 is positioned in the Binchuan sequence among the suites of low-Ti basalts (Xiao *et al.*, 2004), whereas sample EM43 is from within the high-Ti suite, some 1·3 km higher (Xu *et al.*, 2001). There are also other reports of picrites from the Binchuan area; however, their stratigraphic position was not indicated (Song *et al.*, 2001). These picrites are significantly more Ti-rich (Ti/Y = 701–808) than EM43 and WL38, and are a good match to those from the Lijiang (Hanski *et al.*, 2010) and Daju (Zhang *et al.*, 2006*a*) areas (Electronic Appendix 1).

It is worth emphasizing again that sample EM43, the best candidate for the low-Ti primitive melt, is found within a sequence dominated by high-Ti magmas (Xu *et al.*, 2001). Thus, a compositional continuum between the LTi and HTi series to which we have assigned an 'end-member' status reflects a complex interplay between distinct mantle sources, their melting conditions and magma mixing, assimilation and differentiation processes in the crust.

Implications for magma sources

Flood basalt volcanism requires massive melting of the mantle, induced either by strong thermal anomalies (excess temperatures up to ~350°C), or alternatively by lowering of melting temperatures by other components (volatiles or/and compositional heterogeneities produced by the recycling of crustal rocks into the ambient mantle). At present, debate about the petrogenesis of continental flood basalts is still centred on the relative roles of so-called 'mantle plumes' and subcontinental lithospheric mantle. Mantle plumes are considered to generate melt below the lithosphere (mantle plume head melting; e.g. Richards *et al.*, 1989; Campbell & Griffiths, 1990) or cause lithospheric rifting over abnormally hot asthenosphere (mantle plume tail melting; e.g. White & McKenzie, 1989). An alternative to mantle plumes involves melting of hydrated subcontinental lithosphere mantle (e.g. Gallagher & Hawkesworth, 1992; Turner & Hawkesworth, 1995) and basaltic lithologies stored in the upper mantle (e.g. eclogite derived from ancient subducted oceanic crust or delaminated lower crust; Cordery *et al.*, 1997; Anderson, 2005; Lustrino, 2005). All existing models rely on geophysical and whole-rock geochemical constraints, but are affected by a lack of reliable data on the compositions and temperatures of the primary melts. The latter can only be inferred from petrological studies of early formed phenocrysts and their entrapped melt inclusions (e.g. Sobolev, 1996; Sobolev *et al.*, 2007).

The presence of primitive, or near-primitive, high-Mg olivine phenocrysts (Fo > 88 mol %; Fig. 6) in the Emeishan picrites implies that primary melts, equilibrated with the mantle source, were involved in their petrogenesis. Abundances of trace elements (e.g. Ni and Mn; Fig. 7) in the primitive olivines reflect those in the parental melts, and have been used to define the amounts of peridotite and pyroxenite components in the source of the mantle-derived magmas (Sobolev *et al.*, 2007). Partial melts of garnet pyroxenite are enriched in Si and Ni, but poorer in Mg, Ca and Mn than melts of peridotite (Sobolev *et al.*, 2007). In the case of the Emeishan magmatic suites the derivation of the LTi end-member from a garnet-free peridotite source is strongly suggested by the olivine compositions, which are similar to those from oceanic rift magmas, with the highest Mn and lowest Ni contents among terrestrial magmatic olivines (Fig. 7). The olivine compositions from other Emeishan picrites are characterized by lower Mn and higher Ni than the LTi olivine (Fig. 7), indicating changing proportion of olivine and pyroxene in the residual mantle. The mantle sources of the ITi and HTi magmas are calculated to have 21% and 47% of a garnet pyroxenite component, respectively [for the calculation method see Sobolev *et al.* (2008) and Gurenko *et al.* (2010)]. The increasing role of garnet pyroxenite in the source of the Emeishan magmas, other than the LTi end-member (see also He *et al.*, 2010), is consistent with the magnitude of the 'garnet signature' (e.g. Gd/Yb) in the trace element patterns of the ITi and HTi magmas

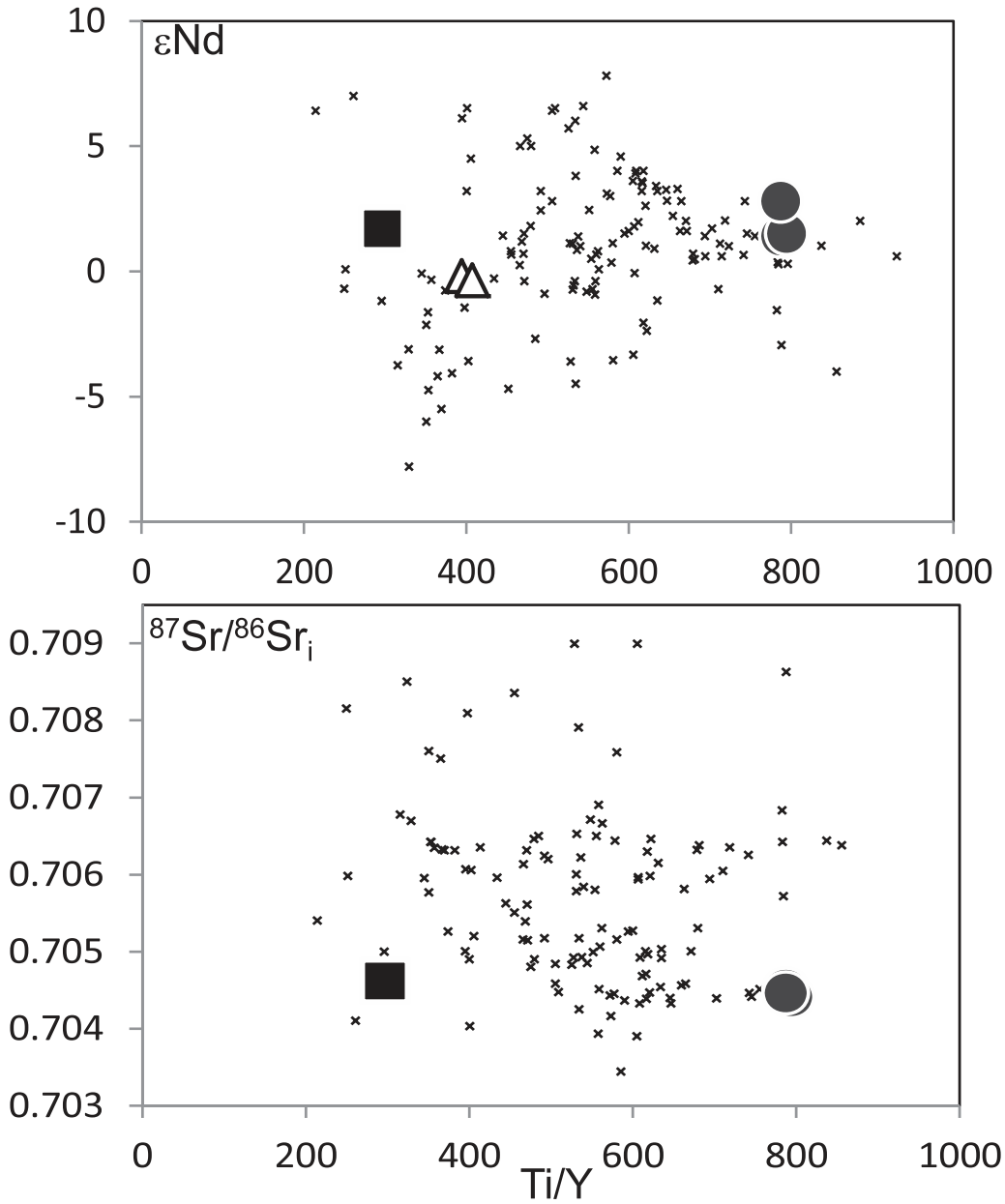

Fig. 11. Nd and Sr isotope compositions of the Emeishan picrites and basalts vs bulk-rock Ti/Y. Symbols and data sources as in Fig. 3. The data for LTi, ITi and HTi picrites are sourced from Xu *et al.* (2001), Hanski *et al.* (2010) and Chung & Jahn (1995), respectively.

(Fig. 5; Hanski *et al.*, 2010). Similarly, the earliest stages of the contemporaneous magmatism forming the Siberian LIP were dominated by an eclogite mantle component with a lower melting temperature, rather than involving low-degree partial melting of a garnet lherzolite source (Sobolev *et al.*, 2009).

Although it is tempting to assign voluminous flood basalt volcanism to melting of exclusively olivine-free, garnet-pyroxenite lithologies in the upwelling asthenosphere and the base of lithosphere, the compositional continuum of the primary melts, inferred from our study of the Emeishan province, may indicate a corresponding continuum in the mantle sources, their depths and degrees of melting. Unfortunately, any approach to quantitatively constrain the mantle sources and melting parameters is impeded by the lack of reliable compositional and temperature data for the primary melts and complications caused by the 'heterogenizing effects' of crustal assimilation and the 'homogenizing effects' of magma mixing.

The differences in radiogenic isotope compositions that have been used in advocating distinct mantle sources for the low-Ti and high-Ti series within a single area

(e.g. Xiao *et al.*, 2004; Xu *et al.*, 2007) are not supported in our study, if the published data for the whole province are considered (Fig. 11). In fact, the classification parameter Ti/Y and the Sr and Nd isotope compositions show no correlation; contrasting LTi and HTi picrites are surprisingly similar to each other and to Bulk Silicate Earth [$^{87}Sr/^{86}Sr_i$ ~0·7045; εNd(t) ~+1·7; Fig. 11]. Such uniform isotope compositions of geochemically different suites imply possible equilibration of their respective mantle sources. Moreover, the more radiogenic Sr and less radiogenic Nd isotopic compositions than those typical of oceanic basalts suggest involvement of the subcontinental mantle lithosphere rather than the convecting asthenosphere or deep mantle 'plumes' [see review by Turner & Hawkesworth (1995)]. Wide geochemical (Figs 3–5 and 10) and isotope ($^{87}Sr/^{86}Sr_i$ 0·7035–0·7090; εNd(t) ~−7 to +7; Fig. 11) variations in a single LIP is an ample warning for caution in future petrological reconstructions of the primary melts and respective mantle sources of continental LIP magmatism.

CONCLUSIONS

Flood basalt magmas in LIPs may provide important information about the thermal and compositional state of the mantle at the time of their eruption, and in some cases about processes of continental break-up, faunal mass extinctions and the formation of major Cu–Ni–PGE sulphide and Fe–Ti–V oxide deposits (e.g. Coffin & Eldholm, 1992; Wignall, 2001; Ernst *et al.*, 2005; Zhou *et al.*, 2008). However, the common focus in the literature on more evolved rocks in a given stratigraphic sequence within a large igneous province may not give a true representation of the petrological and geodynamic characteristics of LIP evolution as a whole. The geochemical characteristics of the primary melts are typically obscured by their interactions with both lithospheric mantle and crustal rocks, crystallization, degassing, and different types of melt immiscibility that may contribute further to the compositional diversity inherited from mantle melting, and pre-eruption mixing of melt batches that tends to average the compositions of the erupted magmas. Different mantle source compositions, melting degrees and depths of melt segregation are usually inferred from bulk-rock compositions; such data are not always critically assessed in the context of the original primary magmas. In contrast, the present study of picritic rocks and their primitive phenocrysts and olivine- and Cr-spinel hosted melt inclusions is shown to be the most effective way of identifying significant variability among the parental melt compositions. Our study of picrites from different parts of the Emeishan LIP provides insights into the continuous spectrum of primary melts that may exist in cratonic settings and calls for combining separately published studies on melt compositions and their stratigraphic relationships. We are concerned that previous reconstructions of mantle sources and melting conditions for contrasting magma types [high-Ti melts produced by low-degree melting of garnet-bearing 'plume' mantle and low-Ti melts derived from high-degree melting of shallower peridotite; e.g. Xu *et al.* (2001) and Ali *et al.* (2005)] are over-simplified and do not reflect the stratigraphic position, radiogenic isotope composition and presence of garnet pyroxenite in the subcontinental lithospheric mantle and upwelling mantle as a potential source of the magmas. Varying proportions of 'peridotite' and 'eclogite' or garnet pyroxenite may exist in the mantle under the continents (Gallagher & Hawkesworth, 1992; Tuff *et al.*, 2005; Melluso *et al.*, 2006; Sobolev *et al.*, 2009) and the ocean basins (Kamenetsky *et al.*, 2001*b*; O'Reilly *et al.*, 2009), and could potentially be responsible for both the volumes and geochemical characteristics of continental flood basalt magmas.

ACKNOWLEDGEMENTS

We are indebted to Tony Crawford, who initiated and supported this study. Thanks are due to P. Robinson, S. Gilbert and K. McGoldrick for performing rock analyses. We are grateful to Alex Sobolev and Eero Hanski for discussion of our results and ideas. Detailed and thoughtful comments by Nick Rogers and an anonymous reviewer, and editorial handling by Simon Turner helped to clarify and improve the paper.

FUNDING

This study was initially (2003–2005) supported by the Alexander von Humboldt Foundation (Germany) in the form of the Wolfgang Paul Award to A. Sobolev and the Friedrich Wilhelm Bessel Award to V. Kamenetsky. Financial support for these studies in 2010–2011 was provided by the University of Tasmania 'New Star' Professorship and an Australian Research Council Discovery Grant to V. Kamenetsky 'Kimberlites and Flood Basalts: Linking Primary Melts with Mantle and Crustal Sources'.

SUPPLEMENTARY DATA

Supplementary data for this paper are available at *Journal of Petrology* online.

REFERENCES

Ali, J. R., Thompson, G. M., Zhou, M. F. & Song, X. Y. (2005). Emeishan large igneous province, SW China. *Lithos* **79**, 475–489.

Anderson, D. L. (2005). Large igneous provinces, delamination, and fertile mantle. *Elements* **1**, 271–275.

Bryan, S. E., Peate, I. U., Peate, D. W., Self, S., Jerram, D. A., Mawby, M. R., Marsh, J. S. & Miller, J. A. (2010). The largest volcanic eruptions on Earth. *Earth-Science Reviews* **102**, 207–229.

Campbell, I. H. & Griffiths, R. W. (1990). Implications of mantle plume structure for the evolution of flood basalts. *Earth and Planetary Science Letters* **99**, 79–93.

Chesley, J. T. & Ruiz, J. (1998). Crust–mantle interaction in large igneous provinces: Implications from the Re–Os isotope systematics of the Columbia River flood basalts. *Earth and Planetary Science Letters* **154**, 1–11.

Chung, S.-L. & Jahn, B.-M. (1995). Plume–lithosphere interaction in generation of the Emeishan flood basalts at the Permian–Triassic boundary. *Geology* **23**, 889–892.

Chung, S.-L., Lee, T.-Y., Lo, C.-H., Wang, P.-L., Chen, C.-Y., Nguyen, T. Y., Tran, T. H. & Wu, G. Y. (1997). Intraplate extension prior to continental extrusion along the Ailao Shan–Red River shear zone. *Geology* **25**, 311–314.

Coffin, M. F. & Eldholm, O. (1992). Volcanism and continental break-up: a global compilation of large igneous provinces. In: Storey, B. C., Alabaster, T. & Pankhurst, R. J. (eds) *Magmatism and the Causes of Continental Break-up. Geological Society, London, Special Publications* **68**, 17–30.

Cordery, M. J., Davies, G. F. & Campbell, I. H. (1997). Genesis of flood basalts from eclogite-bearing mantle plumes. *Journal of Geophysical Research* **102**, 20179–20197.

Cox, K. G. & Jamieson, B. G. (1974). The olivine-rich lavas of Nuanetsi: a study of polybaric magmatic evolution. *Journal of Petrology* **15**, 269–301.

Danyushevsky, L. V. (2001). The effect of small amounts of H_2O on crystallisation of mid-ocean ridge and backarc basin magmas. *Journal of Volcanology and Geothermal Research* **110**, 265–280.

Danyushevsky, L. V., Della-Pasqua, F. N. & Sokolov, S. (2000). Re-equilibration of melt inclusions trapped by magnesian olivine phenocrysts from subduction-related magmas: petrological implications. *Contributions to Mineralogy and Petrology* **138**, 68–83.

Danyushevsky, L. V., McNeill, A. W. & Sobolev, A. V. (2002). Experimental and petrological studies of melt inclusions in phenocrysts from mantle-derived magmas: an overview of techniques, advantages and complications. *Chemical Geology* **183**, 5–24.

Duncan, A. R., Erlank, A. J. & Marsh, J. S. (1984). Regional geochemistry of the Karoo igneous province. *Special Publication of the Geological Society of South Africa* **13**, 355–388.

Ernst, R. E., Buchan, K. L. & Campbell, I. H. (2005). Frontiers in Large Igneous Province research. *Lithos* **79**, 271–297.

Ewart, A., Marsh, J. S., Milner, S. C., Duncan, A. R., Kamber, B. S. & Armstrong, R. A. (2004). Petrology and geochemistry of Early Cretaceous bimodal continental flood volcanism of the NW Etendeka, Namibia. Part 1: Introduction, mafic lavas and re-evaluation of mantle source components. *Journal of Petrology* **45**, 59–105.

Ford, C. E., Russel, D. G., Craven, J. A. & Fisk, M. R. (1983). Olivine–liquid equilibria: temperature, pressure and composition dependence of the crystal/liquid cation partition coefficients for Mg, Fe^{2+}, Ca and Mn. *Journal of Petrology* **24**, 256–265.

Gallagher, K. & Hawkesworth, C. J. (1992). Dehydration melting and generation of continental flood basalts. *Nature* **258**, 57–59.

Gurenko, A. A., Hoernle, K. A., Sobolev, A. V., Hauff, F. & Schmincke, H. U. (2010). Source components of the Gran Canaria (Canary Islands) shield stage magmas: evidence from olivine composition and Sr–Nd–Pb isotopes. *Contributions to Mineralogy and Petrology* **159**, 689–702.

Hanski, E., Kamenetsky, V. S., Luo, Z. Y., Xu, Y. G. & Kuzmin, D. V. (2010). Primitive magmas in the Emeishan Large Igneous Province, southwestern China and northern Vietnam. *Lithos* **119**, 75–90.

He, Q., Xiao, L., Balta, B., Gao, R. & Chen, J. Y. (2010). Variety and complexity of the Late-Permian Emeishan basalts: Reappraisal of plume–lithosphere interaction processes. *Lithos* **119**, 91–107.

Holm, P. M., Gill, R. C. O., Pedersen, A. K., Larsen, J. G., Hald, N., Nielsen, T. F. D. & Thirlwall, M. F. (1993). The Tertiary picrites of West Greenland: contributions from 'Icelandic' and other sources. *Earth and Planetary Science Letters* **115**, 227–244.

Jourdan, F., Bertrand, H., Scharer, U., Blichert-Toft, J., Feraud, G. & Kampunzu, A. B. (2007). Major and trace element and Sr, Nd, Hf and Pb isotope compositions of the Karoo large igneous province, Botswana–Zimbabwe: Lithosphere vs mantle plume contribution. *Journal of Petrology* **48**, 1043–1077.

Kamenetsky, V. (1996). Methodology for the study of melt inclusions in Cr-spinel, and implications for parental melts of MORB from FAMOUS area. *Earth and Planetary Science Letters* **142**, 479–486.

Kamenetsky, V. S., Everard, J. L., Crawford, A. J., Varne, R., Eggins, S. M. & Lanyon, R. (2000). Enriched end-member of primitive MORB melts: petrology and geochemistry of glasses from Macquarie Island (SW Pacific). *Journal of Petrology* **41**, 411–430.

Kamenetsky, V. S., Crawford, A. J. & Meffre, S. (2001*a*). Factors controlling chemistry of magmatic spinel: an empirical study of associated olivine, Cr-spinel and melt inclusions from primitive rocks. *Journal of Petrology* **42**, 655–671.

Kamenetsky, V. S., Maas, R., Sushchevskaya, N. M., Norman, M., Cartwright, I. & Peyve, A. A. (2001*b*). Remnants of Gondwanan continental lithosphere in oceanic upper mantle: Evidence from the South Atlantic Ridge. *Geology* **29**, 243–246.

Kamenetsky, V. S., Sobolev, A. V., Eggins, S. M., Crawford, A. J. & Arculus, R. J. (2002). Olivine-enriched melt inclusions in chromites from a low-Ca boninite, Cape Vogel, Papua New Guinea: evidence for ultramafic primary magma, refractory mantle source and enriched components. *Chemical Geology* **183**, 287–303.

Kamenetsky, V. S., Gurenko, A. A. & Kerr, A. C. (2010). Composition and temperature of komatiite melts from Gorgona Island constrained from olivine-hosted melt inclusions. *Geology* **38**, 1003–1006.

Larsen, L. M. & Pedersen, A. K. (2009). Petrology of the Paleocene picrites and flood basalts on Disko and Nuussuaq, West Greenland. *Journal of Petrology* **50**, 1667–1711.

le Roux, P. J., le Roex, A. P., Schilling, J. G., Shimizu, N., Perkins, W. W. & Pearce, N. J. G. (2002). Mantle heterogeneity beneath the southern Mid-Atlantic Ridge: trace element evidence for contamination of ambient asthenospheric mantle. *Earth and Planetary Science Letters* **203**, 479–498.

Li, J., Xu, J. F., Suzuki, K., He, B., Xu, Y. G. & Ren, Z. Y. (2010). Os, Nd and Sr isotope and trace element geochemistry of the Muli picrites: Insights into the mantle source of the Emeishan Large Igneous Province. *Lithos* **119**, 108–122.

Lightfoot, P. C., Hawkesworth, C. J., Hergt, J., Naldrett, A. J., Gorbachev, N. S., Fedorenko, V. A. & Doherty, W. (1993). Remobilization of the continental lithosphere by a mantle plume—major-element, trace-element, and Sr-isotope, Nd-isotope, and Pb-isotope evidence from picritic and tholeiitic lavas of the Norilsk District, Siberian Trap, Russia. *Contributions to Mineralogy and Petrology* **114**, 171–188.

Lustrino, M. (2005). How the delamination and detachment of lower crust can influence basaltic magmatism. *Earth-Science Reviews* **72**, 21–38.

Melluso, L., Beccaluva, L., Brotzu, P., Gregnanin, A., Gupta, A. K., Morbidelli, L. & Traversa, G. (1995). Constraints on the mantle sources of the Deccan Traps from petrology and geochemistry of the basalts of Gujarat State (Western India). *Journal of Petrology* **36**, 1393–1432.

Melluso, L., Mahoney, J. J. & Dallai, L. (2006). Mantle sources and crustal input as recorded in high-Mg Deccan Traps basalts of Gujarat (India). *Lithos* **89**, 259–274.

Molzahn, M., Reisberg, L. & Wörner, G. (1996). Os, Sr, Nd, Pb, O isotope and trace element data from the Ferrar flood basalts, Antarctica: evidence for an enriched subcontinental lithospheric source. *Earth and Planetary Science Letters* **144**, 529–546.

O'Reilly, S. Y., Zhang, M., Griffin, W. L., Begg, G. & Hronsky, J. (2009). Ultradeep continental roots and their oceanic remnants: A solution to the geochemical 'mantle reservoir' problem? *Lithos* **112**, 1043–1054.

Peate, D. W. & Hawkesworth, C. J. (1996). Lithospheric to asthenospheric transition in low-Ti flood basalts from southern Parana, Brazil. *Chemical Geology* **127**, 1–24.

Peate, D. W., Hawkesworth, C. J. & Mantovani, M. S. M. (1992). Chemical stratigraphy of the Parana lavas (South America): classification of magma types and their spatial distribution. *Bulletin of Volcanology* **55**, 119–139.

Peate, D. W., Hawkesworth, C. J., Mantovani, M. M. S., Rogers, N. W. & Turner, S. P. (1999). Petrogenesis and stratigraphy of the high-Ti/Y Urubici magma type in the Paraná flood basalt province and implications for the nature of 'Dupal'-type mantle in the South Atlantic region. *Journal of Petrology* **40**, 451–473.

Qi, L., Wang, C. Y. & Zhou, M. F. (2008). Controls on the PGE distribution of Permian Emeishan alkaline and peralkaline volcanic rocks in Longzhoushan, Sichuan Province, SW China. *Lithos* **106**, 222–236.

Richards, M. A., Duncan, R. A. & Courtillot, V. (1989). Flood basalts and hotspot tracks: plume heads and tails. *Science* **246**, 103–107.

Shellnutt, J. G. & Jahn, B. M. (2011). Origin of Late Permian Emeishan basaltic rocks from the Panxi region (SW China): Implications for the Ti-classification and spatial–compositional distribution of the Emeishan flood basalts. *Journal of Volcanology and Geothermal Research* **199**, 85–95.

Shellnutt, J. G., Zhou, M. F. & Chung, S. L. (2010). The Emeishan large igneous province: Advances in the stratigraphic correlations and petrogenetic and metallogenic models. Preface. *Lithos* **119**, ix–x.

Sigurdsson, I. A., Kamenetsky, V. S., Crawford, A. J., Eggins, S. M. & Zlobin, S. K. (1993). Primitive island arc and oceanic lavas from the Hunter ridge–Hunter fracture zone. Evidence from glass, olivine and spinel compositions. *Mineralogy and Petrology* **47**, 149–169.

Sobolev, A. V. (1996). Melt inclusions in minerals as a source of principal petrological information. *Petrology* **4**, 228–239.

Sobolev, A. V., Hofmann, A. W., Kuzmin, D. V., Yaxley, G. M., Arndt, N. T., Chung, S.-L., Danyushevsky, L. V., Elliott, T., Frey, F. A., Garcia, M. O., Gurenko, A. A., Kamenetsky, V. S., Kerr, A. C., Krivolutskaya, N. A., Matvienkov, V. V., Nikogosian, I. K., Rocholl, A., Sigurdsson, I. A., Sushchevskaya, N. M. & Teklay, M. (2007). The amount of recycled crust in sources of mantle-derived melts. *Science* **316**, 412–417.

Sobolev, A. V., Hofmann, A. W., Brugmann, G., Batanova, V. G. & Kuzmin, D. V. (2008). A quantitative link between recycling and osmium isotopes. *Science* **321**, 536–536.

Sobolev, A. V., Krivolutskaya, N. A. & Kuzmin, D. V. (2009). Petrology of the parental melts and mantle sources of Siberian trap magmatism. *Petrology* **17**, 253–286.

Song, X. Y., Zhou, M. F., Hou, Z. Q., Cao, Z. M., Wang, Y. L. & Li, Y. G. (2001). Geochemical constraints on the mantle source of the upper Permian Emeishan continental flood basalts, southwestern China. *International Geology Review* **43**, 213–225.

Song, X. Y., Zhou, M. F., Cao, Z. M., Sun, M. & Wang, Y. L. (2003). Ni–Cu–(PGE) magmatic sulfide deposits in the Yangliuping area, Permian Emeishan Igneous province, SW China. *Mineralium Deposita* **38**, 831–843.

Song, X. Y., Zhou, M. F., Cao, Z. M. & Robinson, P. T. (2004). Late Permian rifting of the South China Craton caused by the Emeishan mantle plume? *Journal of the Geological Society, London* **161**, 773–781.

Song, X. Y., Zhou, M. F., Keays, R. R., Cao, Z. M., Sun, M. & Qi, L. (2006). Geochemistry of the Emeishan flood basalts at Yangliuping, Sichuan, SW China: implications for sulfide segregation. *Contributions to Mineralogy and Petrology* **152**, 53–74.

Song, X. Y., Qi, H. W., Robinson, P. T., Zhou, M. F., Cao, Z. M. & Chen, L. M. (2008). Melting of the subcontinental lithospheric mantle by the Emeishan mantle plume; evidence from the basal alkaline basalts in Dongchuan, Yunnan, Southwestern China. *Lithos* **100**, 93–111.

Sun, S.-S. & McDonough, W. F. (1989). Chemical and isotopic systematics of oceanic basalts: implications for mantle composition and processes. In: Saunders, A. D. & Norry, M. J. (eds) *Magmatism in the Ocean Basins. Geological Society, London, Special Publications* **42**, 313–345.

Sun, W. D., Hu, Y. H., Kamenetsky, V. S., Eggins, S. M., Chen, M. & Arculus, R. J. (2008). Constancy of Nb/U in the mantle revisited. *Geochimica et Cosmochimica Acta* **72**, 3542–3549.

Sweeney, R. J., Falloon, T. J., Green, D. H. & Tatsumi, Y. (1991). The mantle origins of Karoo picrites. *Earth and Planetary Science Letters* **107**, 256–271.

Sweeney, R. J., Duncan, A. R. & Erlank, A. J. (1994). Geochemistry and petrogenesis of central Lebombo basalts of the Karoo Igneous Province. *Journal of Petrology* **35**, 95–125.

Tran, V. A., Pang, K.-N., Chung, S.-L., Lin, H.-M., Hoa, T. T., Anh, T. T. & Yang, H. J. (2011). Geochemical and Sr–Nd isotopic constraints on Permian intra-plate volcanism in the Song Da zone (NW Vietnam). *Journal of Asian Earth Sciences* **42**, 1341–1355.

Tuff, J., Takahashi, E. & Gibson, S. A. (2005). Experimental constraints on the role of garnet pyroxenite in the genesis of high-Fe mantle plume derived melts. *Journal of Petrology* **46**, 2023–2058.

Turner, S. & Hawkesworth, C. (1995). The nature of sub-continental mantle: constraints from the major-element composition of continental flood basalts. *Chemical Geology* **120**, 295–314.

Wang, C. Y., Zhou, M. F. & Qi, L. (2007). Permian flood basalts and mafic intrusions in the Jinping (SW China) Song Da (northern Vietnam) district: Mantle sources, crustal contamination and sulfide segregation. *Chemical Geology* **243**, 317–343.

White, R. & McKenzie, D. (1989). Magmatism at rift zones: the generation of volcanic continental margins and flood basalts. *Journal of Geophysical Research* **94**, 7685–7729.

Wignall, P. B. (2001). Large igneous provinces and mass extinctions. *Earth-Science Reviews* **53**, 1–33.

Xiao, L., Xu, Y. G., Chung, S. L., He, B. & Mei, H. J. (2003). Chemostratigraphic correlation of Upper Permian lavas from Yunnan province, China: Extent of the Emeishan Large Igneous Province. *International Geology Review* **45**, 753–766.

Xiao, L., Xu, Y. G., Mei, H. J., Zheng, Y. F., He, B. & Pirajno, F. (2004). Distinct mantle sources of low-Ti and high-Ti basalts from the western Emeishan large igneous province, SW China: implications for plume–lithosphere interaction. *Earth and Planetary Science Letters* **228**, 525–546.

Xu, J. F., Suzuki, K., Xu, Y. G., Mei, H. J. & Li, J. (2007). Os, Pb, and Nd isotope geochemistry of the Permian Emeishan continental flood basalts: Insights into the source of a large igneous province. *Geochimica et Cosmochimica Acta* **71**, 2104–2119.

Xu, Y. G., Chung, S. L., Jahn, B. M. & Wu, G. Y. (2001). Petrologic and geochemical constraints on the petrogenesis of Permian–Triassic Emeishan flood basalts in southwestern China. *Lithos* **58**, 145–168.

Xu, Y. G., Luo, Z. Y., Huang, X. L., He, B., Xiao, L., Xie, L. W. & Shi, Y. R. (2008). Zircon U–Pb and Hf isotope constraints on crustal melting associated with the Emeishan mantle plume. *Geochimica et Cosmochimica Acta* **72**, 3084–3104.

Yaxley, G. M., Kamenetsky, V. S., Kamenetsky, M., Norman, M. D. & Francis, D. (2004). Origins of compositional heterogeneity in olivine-hosted melt inclusions from the Baffin Island picrites. *Contributions to Mineralogy and Petrology* **148**, 426–442.

Zhang, Z. C., Mahoney, J. J., Mao, J. W. & Wang, F. H. (2006*a*). Geochemistry of picritic and associated basalt flows of the western Emeishan flood basalt province, China. *Journal of Petrology* **47**, 1997–2019.

Zhang, Z. C., Mahoney, J. J., Wang, F. S., Zhao, L., Ai, Y. & Yang, T. Z. (2006*b*). Geochemistry of picritic and associated basalt flows of the western Emeishan flood basalt province, China: evidence for a plume-head origin. *Acta Petrologica Sinica* **22**, 1538–1552.

Zhou, M. F., Malpas, J., Song, X. Y., Robinson, P. T., Sun, M., Kennedy, A. K., Lesher, C. M. & Keays, R. R. (2002). A temporal link between the Emeishan large igneous province (SW China) and the end-Guadalupian mass extinction. *Earth and Planetary Science Letters* **196**, 113–122.

Zhou, M. F., Arndt, N. T., Malpas, J., Wang, C. Y. & Kennedy, A. K. (2008). Two magma series and associated ore deposit types in the Permian Emeishan large igneous province, SW China. *Lithos* **103**, 352–368.